

3D Triple-resonance NMR techniques for the sequential assignment of NH and ^{15}N resonances in ^{15}N - and ^{13}C -labelled proteins

Rüdiger Weisemann^a, Heinz Rüterjans^{a,*} and Wolfgang Bermel^b

^a*Institut für Biophysikalische Chemie der Johann Wolfgang Goethe Universität, D-6000 Frankfurt am Main, Germany*

^b*Bruker Analytische Messtechnik GmbH, D-7512 Karlsruhe/Rheinstetten, Germany*

Received 2 November 1992

Accepted 4 November 1992

Keywords: 3D NMR; J connectivity; Sequential assignment; Isotope labelling; Proteins; Ribonuclease T1

SUMMARY

Two new 3D ^1H - ^{15}N - ^{13}C triple-resonance experiments are presented which provide sequential cross peaks between the amide proton of one residue and the amide nitrogen of the preceding and succeeding residues or the amide proton of one residue and the amide proton of the preceding and succeeding residues, respectively. These experiments, which we term 3D-HN(CA)NNH and 3D-H(NCA)NNH, utilize an optimized magnetization transfer via the $^2J_{\text{NC}\alpha}$ coupling to establish the sequential assignment of backbone NH and ^{15}N resonances. In contrast to NH–NH connectivities observable in homonuclear NOESY spectra, the assignments from the 3D-H(NCA)NNH experiment are conformation independent to a first-order approximation. Thus the assignments obtained from these experiments can be used as either confirmation of assignments obtained from a conventional homonuclear approach or as an initial step in the analysis of backbone resonances according to Ikura et al. (1990) [*Biochemistry*, **29**, 4659–4667]. Both techniques were applied to uniformly ^{15}N - and ^{13}C -labelled ribonuclease T1.

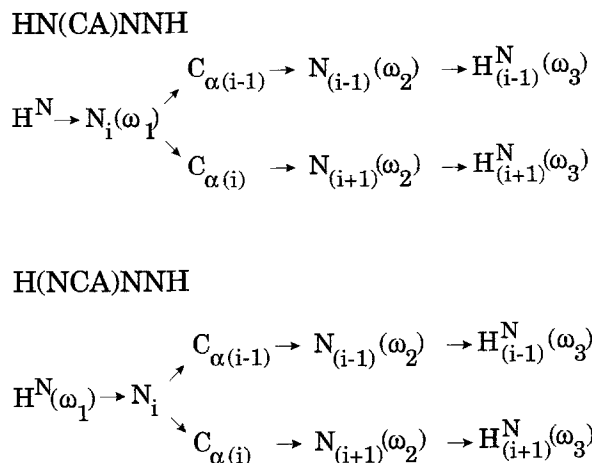
Complete sequential assignment of the backbone resonances of a protein is a crucial step in the analysis of its solution structure. For proton resonances, this is normally achieved by following the conventional assignment procedure using COSY, TOCSY and NOESY experiments to establish intra-residual and inter-residual connectivities (Kumar et al. 1980; Wagner and Wüthrich, 1982; Bax and Davis, 1985). For larger proteins, this approach has been shown to be limited by several serious drawbacks, such as increasing linewidths and spectral overlap. Especially in NOESY spectra of larger proteins, the limited resolution and spectral overlap may lead to difficulties in the assignment of sequential connectivities. Several techniques have been introduced to obtain sequential assignments in either ^{15}N -labelled proteins (three-dimensional (3D) ^{15}N dispersed NOESY and TOCSY experiments; Fesik and Zuiderweg, 1988; Marion et al.,

*To whom correspondence should be addressed.

1989a,b) or in proteins labelled uniformly with ^{15}N and ^{13}C (3D and 4D triple resonance techniques; Ikura et al. 1990a,b; Bax et al., 1991; Kay et al., 1991, 1992; Wagner et al., 1991; Boucher et al. 1992; Clubb et al., 1992a,b).

These new experiments rely upon one- or two-bond heteronuclear J couplings to transfer magnetization from one nucleus to another, and are thus independent of the conformation adopted by the molecule (Montelione and Wagner, 1989, 1990), whereas the corresponding cross peaks in conventional proton experiments depend on small homonuclear ^3J couplings or on inter-proton distances determined by the tertiary structure of the peptide fragment. Nevertheless, a combination of several triple-resonance experiments and a ^{15}N -TOCSY-HMQC spectrum is needed to achieve sequential assignment of NH and nitrogen resonances using the approach of Ikura et al. (1990a,b).

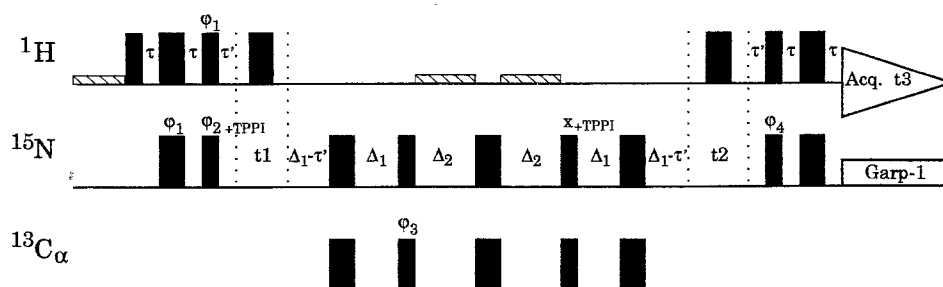
In this study we present two new triple-resonance experiments which directly correlate amide proton or nitrogen resonances in a conformation-independent manner, using one- and two-bond NC_α couplings. The assignments obtained from these experiments can thus be used as starting point for the analysis of homonuclear or ^{15}N -dispersed NOESY spectra. According to the convention introduced by Kay et al. (1991), we term the experiments $\text{HN}(\text{CA})\text{NNH}$ and $\text{H}(\text{NCA})\text{NNH}$, respectively. Thus, these experiments have been designed to yield coherence transfer pathways denoted by a symbolic description as follows:



The pulse sequences used in these experiments are shown in Fig. 1. Both experiments detect the NH proton resonance during the t_3 -acquisition period and therefore must be performed in aqueous solution. With the carrier frequency set at the centre of the amide proton region, suppression of the intense H_2O resonance is achieved by application of a DANTE-type pulse train (Freeman and Morris, 1978; Kay et al., 1989) during the relaxation period.

The experiments only differ in the evolution period, t_1 : evolution of the chemical shifts of the originating nitrogen spin in the $\text{HN}(\text{CA})\text{NNH}$ experiment and evolution of the chemical shifts of the originating amide protons in the $\text{H}(\text{NCA})\text{NNH}$ experiment, respectively. Thus only the relevant magnetization-transfer steps of the $\text{HN}(\text{CA})\text{NNH}$ experiment will be outlined briefly in terms of the operator formalism described by Sørensen et al. (1983).

a) HN(CA)NNH



b) H(NCA)NNH

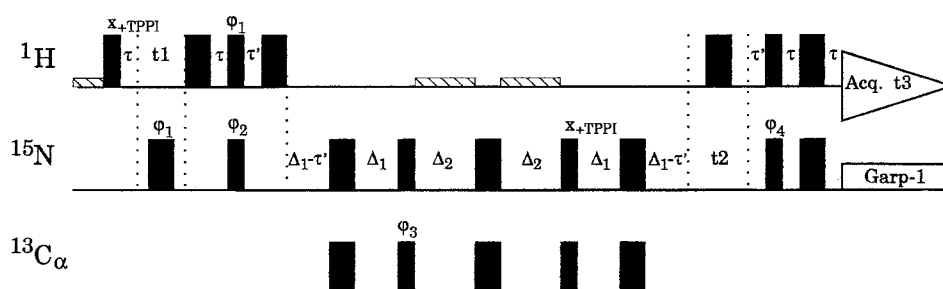


Fig. 1. Pulse sequences for the HN(CA)NNH (a) and the H(NCA)NNH (b) experiments. Narrow and wide bars resemble 90° and 180° pulses, respectively. Pulses where the phases are not indicated were applied along the x axis only. Low hatched bars indicate water suppression using an off-resonance DANTE-type pulse train (Kay et al., 1989). The RF power of the pulses on the C_α -channel was adjusted to assure minimum excitation of the carbonyl spins. Typical delay durations used in these experiments are $\tau = 2.25$ ms, $\tau' = 2.25$ ms, $\Delta_1 = 30$ ms, $\Delta_2 = 50$ ms. The phase cycling used is as follows: $\phi_1 = 2(y), 2(-y)$; $\phi_2 = x, -x$; $\phi_3 = 4(x), 4(-x)$; $\phi_4 = 8(x), 8(-x)$; Acq. = $x, 2(-x), x, 2(-x), 2(x), -x, x, 2(-x), x$. Quadrature detection in both the t_1 and t_2 dimensions was achieved with the TPPI method.

The experiment essentially consists of several INEPT steps (Morris and Freeman, 1979; Morris, 1980) to achieve polarization transfer on the desired pathway in the backbone coupling network. The modularity of the entire experiment requires optimization of each transfer step to select for certain coherence transfer pathways.

Starting with an INEPT sequence, magnetization originating from the NH protons is transferred to the directly bound ^{15}N spin. During the evolution period, t_1 , ^{15}N -magnetization evolves under the ^{15}N chemical shift, ^1H decoupling being achieved by the application of a 180° pulse at the midpoint of t_1 . Both the N-C' and the N-C $_\alpha$ one-bond couplings are active during t_1 but have been neglected because of their small values and the limited resolution in the nitrogen dimension with a typical t_1^{max} of 16 ms. The same holds true for the second nitrogen evolution period, t_2 . By using a second INEPT-type transfer from nitrogen to carbon, the in-phase magnetization ($-S_x$) residing on the ^{15}N spins is transferred into antiphase magnetization with respect to the $^{13}\text{C}_\alpha$ spin of the same residue [$C'_\alpha(i)$] ($^1J_{\text{NC}\alpha} = 7\text{--}11$ Hz, $\Delta_1 = 1/(4^1J_{\text{NC}\alpha})$), as well as to the $^{13}\text{C}'_\alpha$ spin of the

preceding residue [$C\alpha(i-1)$] via the ${}^2J_{NC\alpha}$ coupling (${}^2J_{NC\alpha} = 3-8$ Hz). During the following delays ($2\Delta_2$), the active coupling is refocused, while the coupling to the ${}^{15}N$ spin of the following [$N(i+1)$, (${}^2J_{NC\alpha}$)] or preceding residue [$N(i-1)$, (${}^1J_{NC\alpha}$)] evolves. Refocusing of chemical shifts is accomplished by applying two simultaneous 180° pulses. Reversing the second INEPT step, the resulting ${}^{15}N$, ${}^{13}C_\alpha$ antiphase magnetization is then transferred back into in-phase nitrogen magnetization on different nitrogen spins, and is amplitude-modulated by a product of sine and cosine functions depending on the size of the relevant coupling constants and the evolution delays, Δ_1 and Δ_2 .

With the difference between the coupling constants being only 3 to 5 Hz, the evolution of magnetization during these intervals can never be restricted to a single transfer pathway along the chain of coupled spins, and only the sum of transfers may be calculated to minimize the contribution of the undesired coherence transfer pathway leading to auto-correlation signals (i.e. intra-residual NH-N connectivities).

Just before the t_2 evolution time in the HN(CA)NNH experiment, the effective terms (S denoting the operator for nitrogen nuclei) may be written as:

$$\begin{aligned} \sigma = & \{S_{ix}\cos(\omega_N t_1) \cos(\pi^1 J_{CN}\Delta_1) \sin(\pi^2 J_{CN}\Delta_1) \cos(\pi^1 J_{CN}\Delta_2) \cos(\pi^2 J_{CN}\Delta_2) \cos(\pi^1 J_{CN}\Delta_1) \sin(\pi^2 J_{CN}\Delta_1) \\ & + S_{yx}\cos(\omega_N t_1) \sin(\pi^1 J_{CN}\Delta_1) \cos(\pi^2 J_{CN}\Delta_1) \cos(\pi^1 J_{CN}\Delta_2) \cos(\pi^2 J_{CN}\Delta_2) \sin(\pi^1 J_{CN}\Delta_1) \cos(\pi^2 J_{CN}\Delta_1) \\ & + S_{i-x}\cos(\omega_N t_1) \sin(\pi^1 J_{CN}\Delta_1) \cos(\pi^2 J_{CN}\Delta_1) \sin(\pi^1 J_{CN}\Delta_2) \sin(\pi^2 J_{CN}\Delta_2) \cos(\pi^1 J_{CN}\Delta_1) \sin(\pi^2 J_{CN}\Delta_1) \\ & + S_{i+x}\cos(\omega_N t_1) \cos(\pi^1 J_{CN}\Delta_1) \sin(\pi^2 J_{CN}\Delta_1) \sin(\pi^1 J_{CN}\Delta_2) \sin(\pi^2 J_{CN}\Delta_2) \sin(\pi^1 J_{CN}\Delta_1) \cos(\pi^2 J_{CN}\Delta_1)\} \end{aligned}$$

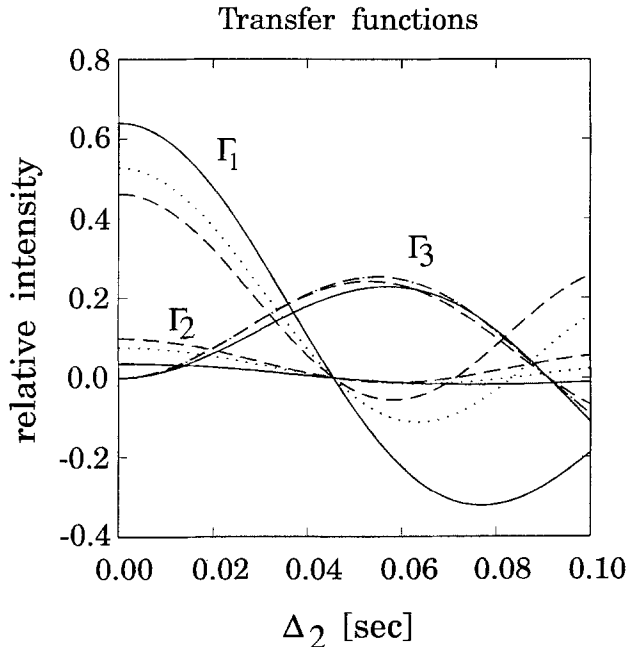


Fig. 2. Simulated transfer functions for intra-residual (Γ^1 , Γ^2) and sequential (Γ^3) cross peaks. The values of the equations given in the text were plotted against Δ_2 . For the calculations a ${}^1J_{NC\alpha}$ coupling constant of 11 Hz was assumed at a delay of $\Delta_1 = 30$ ms. The transfer functions were calculated for three values of the ${}^2J_{NC\alpha}$ coupling constant (Bystrov, 1976): 4 Hz (dashed lines), 6 Hz (dotted lines) and 7 Hz (solid lines)

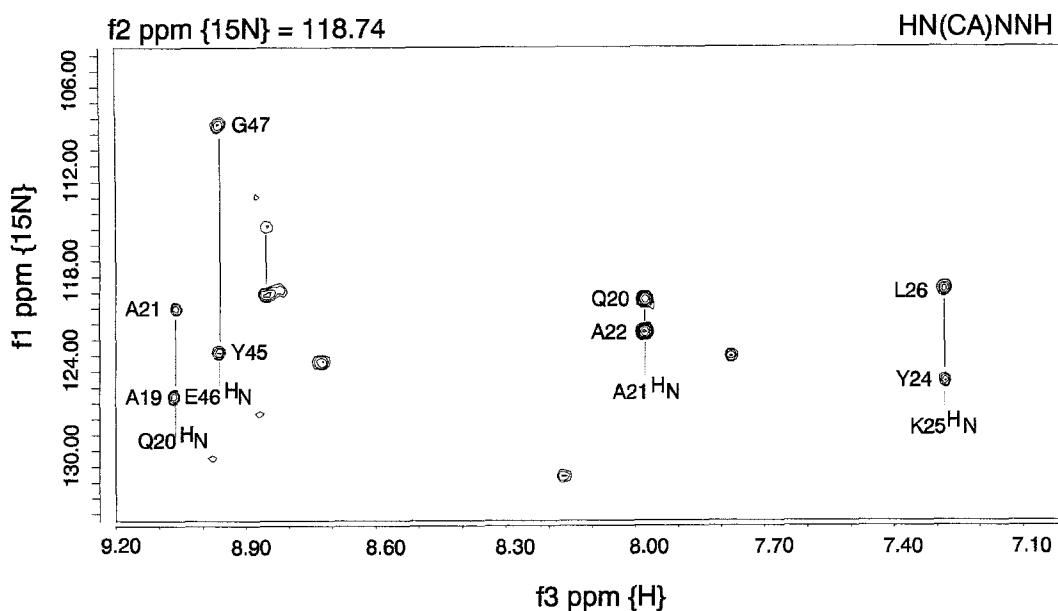


Fig. 3. ω_1 - ω_3 cross plane from a 3D-HN(CA)NNH spectrum recorded with a 3 mM solution of uniformly ^{15}N - and ^{13}C -labelled ribonuclease T1, pH 5.4, in 95% H_2O , 5% D_2O , 308 K. The cross plane was taken in the vicinity of the ^{15}N resonance frequencies of Q20, E46 and A21. The sequential assignment of the nitrogen chemical shifts of the neighbouring amino acids is indicated for these residues. The spectrum was recorded on an unmodified Bruker AMX-600 NMR spectrometer equipped with a multichannel interface and a triple-resonance probe tuned for ^1H , ^{15}N and ^{13}C . C_α pulses were applied at a frequency corresponding to 58 ppm; the RF power was adjusted to give a 90° pulse of 54 μs (yielding minimum excitation of the carbonyl resonances at a ^{13}C spectrometer frequency of 150.9 MHz). GARP-1 decoupling was applied during acquisition using an RF power of 1.2 kHz. The time domain data consisted of 64, 64 and 1024 real data points in the t_1 , t_2 and t_3 dimensions, respectively. The spectrum was recorded in 24 h using a minimum phase cycle of 16 scans. The data were processed employing linear prediction in the t_1 time domain from 64 to 96 points. Additional zero-filling in all dimensions resulted in a data set of $128 \times 64 \times 1024$ (t_1, t_2, t_3) data points. Data processing was done with the TRITON software package (Triton 3Vision, 1991).

The four operators in σ lead to the evolution of three different chemical shifts in the evolution period, t_2 , namely those of the amide nitrogen of residues $i-1$, i and $i+1$, respectively. After t_2 , this magnetization is transferred back from the nitrogen spins to their directly attached protons, reversing the initial INEPT transfer. The back transfer leads to three signals which can be observed in the final spectrum: $f1(^{15}\text{N}_i)f2(^{15}\text{N}_i)f3(\text{NH}_i)$ (diagonal peaks); $f1(^{15}\text{N}_i)f2(^{15}\text{N}_{i-1})f3(\text{NH}_{i-1})$ and $f1(^{15}\text{N}_i)f2(^{15}\text{N}_{i+1})f3(\text{NH}_{i+1})$. In the corresponding H(NCA)NNH experiment the following correlations can be observed: $f1(\text{NH}_i)f2(^{15}\text{N}_i)f3(\text{NH}_i)$ (diagonal peaks); $f1(\text{NH}_i)f2(^{15}\text{N}_{i-1})f3(\text{NH}_{i-1})$ and $f1(\text{NH}_i)f2(^{15}\text{N}_{i+1})f3(\text{NH}_{i+1})$.

As there are two possible pathways leading to diagonal peaks, two transfer functions have to be used to calculate their intensities in the final spectrum, whereas only one transfer function describes the intensity of the two cross-correlated signals. Using product operator formalism and

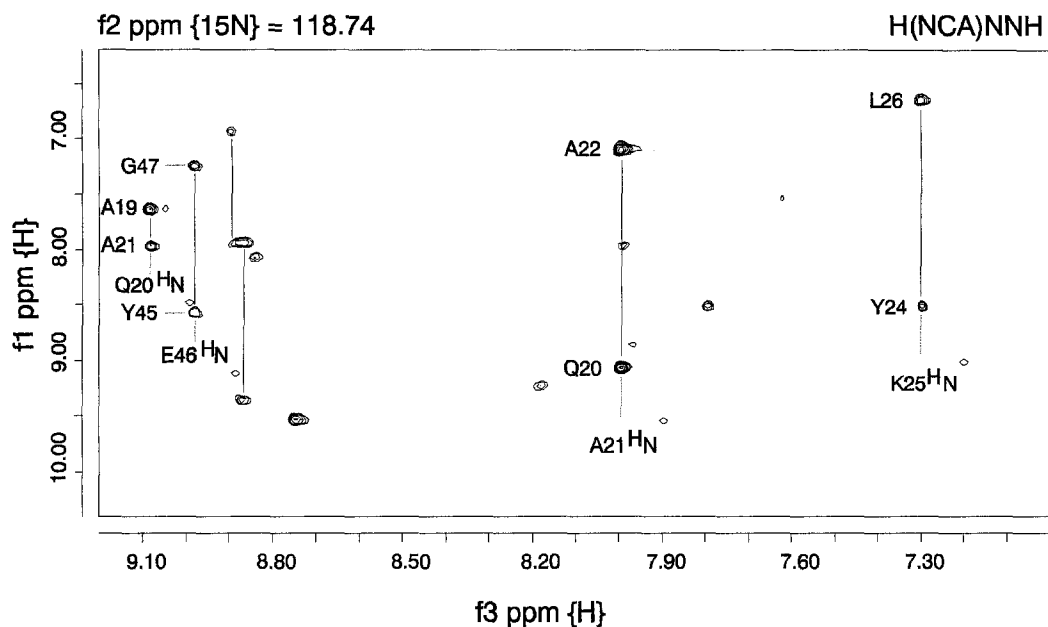


Fig. 4. ω_1 – ω_3 cross plane from a 3D-H(NCA)NNH spectrum recorded with the same sample as in Fig. 3. The sequential assignment of several NH protons is indicated by vertical lines. The experimental parameters were the same as used for the corresponding HN(CA)NNH spectrum except for the size of the t_1 time domain. Before processing, the time domain data comprised 192, 64 and 1024 data points in the t_1 , t_2 and t_3 dimensions, respectively. Owing to the higher resolution required in the t_1 domain, data acquisition took approximately 70 h using a 16-scan phase cycle. The final data set consisted of $512 \times 64 \times 1024$ data points.

neglecting chemical shift evolution during the evolution periods, t_1 and t_2 , the following equations are obtained:

For the diagonal peaks:

$$\Gamma_{\text{dia}}^1 = \cos^2(\pi^1 J_{\text{CN}} \Delta_1) \sin^2(\pi^2 J_{\text{CN}} \Delta_1) \cos(\pi^1 J_{\text{CN}} \Delta_2) \cos(\pi^2 J_{\text{CN}} \Delta_2)$$

$$\Gamma_{\text{dia}}^2 = \sin^2(\pi^1 J_{\text{CN}} \Delta_1) \cos^2(\pi^2 J_{\text{CN}} \Delta_1) \cos(\pi^1 J_{\text{CN}} \Delta_2) \cos(\pi^2 J_{\text{CN}} \Delta_2)$$

For the cross peaks:

$$\Gamma_{\text{cross}}^3 = \cos(\pi^1 J_{\text{CN}} \Delta_1) \cos(\pi^2 J_{\text{CN}} \Delta_1) \sin(\pi^1 J_{\text{CN}} \Delta_1) \cos(\pi^2 J_{\text{CN}} \Delta_1) \sin(\pi^1 J_{\text{CN}} \Delta_2) \sin(\pi^2 J_{\text{CN}} \Delta_2),$$

where T_2 relaxation during the delays has been omitted. The relative intensities calculated from these equations are depicted in Fig. 2 and depend on the delay, Δ_2 . Parameters used in the calculation are given in the legend to Fig. 2.

The tuning of the τ and τ' delays in the sequences of Fig. 1 is trivial. Therefore, the initial and last transfer steps from the NH to the directly bound ^{15}N have been omitted, i.e. optimum transfer has been assumed for these steps. It is obvious from Fig. 2 that the relative intensities of the diagonal signals are minimal in the range of 40–70 ms for Δ_2 , unlike the intensities of the

cross-correlated signals, which are at maximum for a delay duration of approximately 55 ms. Thus maximum intensity for sequential correlations is expected for a delay duration of 55 ms, whereas, depending on both the one-bond and two-bond coupling constants, the diagonal signals have zero intensity at a duration of approximately 45 ms for Δ_2 . The choice of Δ_2 in the range of 45 to 55 ms is therefore subject to experimental optimization with respect to transverse relaxation rather than transfer efficiency.

Figures 3 and 4 show ω_1 – ω_3 cross planes from the two experiments recorded with a 3 mM sample of ribonuclease T1. The cross planes are taken at the ^{15}N resonance frequency of several amino acids and contain sequential cross peaks which are connected by vertical lines. The assignment is indicated in the spectra. More than 90% of the sequential cross peaks could be assigned in the preliminary analysis of the data starting from resonance data obtained from a ^{15}N , ^1H -HSQC (Bodenhausen and Ruben, 1980) spectrum. Despite the lack of information about directionality provided by both experiments, sequential assignment of the resonances is possible due to the uniqueness of a single threefold pattern of peak positions in a successive triple of amide nitrogen or hydrogen atoms. A schematic view of assignment procedure is depicted in Fig. 5. Because of the redundancy of the peak data obtained from the HN(CA)NNH, H(NCA)NNH, ^{15}N -TOCSY-HMQC, ^{15}N -NOESY-HMQC (Marion et al., 1989a) and HMQC-NOESY-HMQC (Frenkiel et al., 1990; Ikura et al., 1990a) spectra, analysis of the peak data of these spectra reduces the ambiguity in the assignment of sequential correlations. The results obtained from this procedure are fully consistent with the results obtained by analysis of backbone resonances using the approach described by Ikura et al. (1990a) applied to ribonuclease T1 (Weisemann, R., unpublished results).

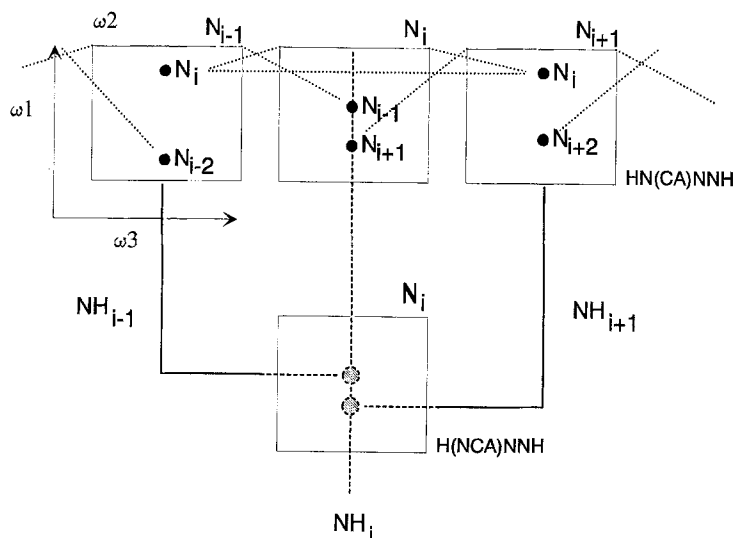


Fig. 5. Schematic description of the sequential assignment procedure with a combination of HN(CA)NNH and H(NCA)NNH peak data. Dotted lines correspond to equal resonance frequencies or coordinates in terms of the 3D spectrum. Data analysis was done by automated peak-picking, sorting of peak coordinates and searching for correlated triples of coordinates. The sequential assignment of nitrogen resonances was then compared to number triples from the H(NCA)NNH spectrum, as well as with a list of auto-correlation peaks obtained from a ^{15}N , ^1H -HSQC spectrum (data not shown). A semi-automatic 'search and compare' procedure is currently being investigated.

The information obtained from both experiments can thus be used in combination with information provided by other correlation experiments in which either the amide nitrogen or the amide proton is correlated with other directly attached or remote nuclei. The 3D-H(NCA)NNH experiment can be applied in combination with either 2D or 3D HMQC-NOESY or homonuclear NOESY spectra to establish sequential assignment of NH–NH connectivities because it directly yields cross peaks ($\text{NH}_i, \text{NH}_{i-1}$) observed typically in such spectra independently of the spatial distance, therefore separating assignment from distance information. The results from a 3D-HN(CA)NNH experiment can be combined with those obtained from 3D-HMQC-TOCSY, 3D-HNCA, 3D-HNCO and 3D-HN(CO)CA spectra to establish the sequential assignment of the nitrogen and carbon backbone resonances. In less ideal cases, for example where not all experiments have been performed, recording of just one of these new experiments in combination with a ^{15}N , ^1H -HSQC spectrum and a NOESY-HMQC spectrum may be sufficient to track most of the sequential backbone ^{15}N or NH resonances, leading to important information in a convenient manner.

ACKNOWLEDGEMENTS

We thank Harald Thüring for the preparation of the ^{15}N -, ^{13}C -labelled sample of ribonuclease T1. We thank the Deutsche Forschungsgemeinschaft for a grant (RU 145/8-6).

REFERENCES

- Bax, A. and Davies, D.G. (1985) *J. Magn. Reson.*, **65**, 335–360.
- Bax, A. Ikura, M., Kay, L.E., Torchia, D.A. and Tschudin, R. (1990) *J. Magn. Reson.*, **86**, 304–318.
- Bax, A. and Ikura, M. (1991) *J. Biomol. NMR*, **1**, 99–104.
- Bodenhausen, G. and Ruben, D.J. (1980) *Chem. Phys. Lett.*, **69**, 185–188.
- Boucher, W., Laue, E.D., Campbell-Burk, S. and Domaille, P.J. (1992) *J. Am. Chem. Soc.*, **114**, 2262–2264.
- Bystrov, V.F. (1976) *Prog. NMR Spectrosc.*, **10**, 41–81.
- Clubb, R.T., Thanabal, V. and Wagner, G. (1992a) *J. Biomol. NMR*, **2**, 203–210.
- Clubb, R.T. and Wagner, G. (1992b) *J. Biomol. NMR*, **2**, 389–394.
- Fesik, S.W. and Zuiderweg, E.R.P. (1988) *J. Magn. Reson.*, **78**, 588–593.
- Frenkiel, T., Bauer, C., Carr, M.D., Birdsall, B. and Feney (1990) *J. Magn. Reson.*, **96**, 420–425.
- Ikura, M., Bax, A., Clore, G.M. and Gronenborn, A.M. (1990a) *J. Am. Chem. Soc.*, **112**, 9020–9022.
- Ikura, M., Kay, L.E. and Bax, A. (1990b) *Biochemistry*, **29**, 4659–4667.
- Kay, L.E., Marion, D. and Bax, A. (1989) *J. Magn. Reson.*, **84**, 72–84.
- Kay, L.E., Ikura, M. and Bax, A. (1991) *J. Magn. Reson.*, **91**, 84–92.
- Kay, L.E., Wittekind, M., McCoy, M.A., Friedrichs, M.S. and Mueller, L. (1992) *J. Magn. Reson.*, **98**, 443–450.
- Kumar, A., Wagner, G., Ernst, R.R. and Wüthrich, K. (1980) *Biochem. Biophys. Res. Commun.*, **96**, 1156–1163.
- Marion, D., Driscoll, P.C., Kay, L.E., Wingfield, P.T. and Bax, A. (1989a), *Biochemistry*, **28**, 6150–6156.
- Marion, D., Kay, L.E., Sparks, S.W., Torchia, D.A. and Bax, A. (1989b), *J. Am. Chem. Soc.*, **111**, 1515–1517.
- Montelione, G.T. and Wagner, G. (1989) *J. Am. Chem. Soc.*, **111**, 5474–5475.
- Montelione, G.T. and Wagner, G. (1990) *J. Magn. Reson.*, **87**, 183–188.
- Morris, G.A. and Freeman, R. (1978) *J. Magn. Reson.*, **29**, 433–462.
- Morris, G.A. and Freeman, R. (1979) *J. Am. Chem. Soc.*, **101**, 760–762.
- Morris, G.A. (1980) *J. Magn. Reson.*, **41**, 185–188.
- Sørensen, O.W., Eich, G.W., Levitt, M.H., Bodenhausen, G. and Ernst, R.R. (1983) *Prog. NMR Spectrosc.*, **89**, 496–514.
- Triton, 3Vision, Department of Chemistry, Utrecht University, (1990).
- Wagner, G. and Wüthrich, K. (1982) *J. Mol. Biol.*, **155**, 347–366.
- Wagner, G., Schmieder, P. and Thanabal, V. (1991) *J. Magn. Reson.*, **93**, 436–440.